Utility of *N*-Methylimidazole in Isolating Crystalline Lanthanide Iodide and Hydroxide Complexes: Crystallographic Characterization of Octasolvated $[Sm(N\text{-MeIm})_8]I_3$ and Polymetallic $[SmI(\mu\text{-}I)(N\text{-MeIm})_3]_2$, $[(N\text{-MeIm})_5Sm(\mu\text{-}OH)]_2I_4$, and $\{[(N\text{-MeIm})_4Sm(\mu\text{-}OH)]_3(\mu_3\text{-}OH)_2\}I_4$

William J. Evans,* Gerd W. Rabe, and Joseph W. Ziller

Department of Chemistry, University of California, Irvine, California 92717

*Received October 7, 1993**

$SmI_2(THF)_2$ reacts in THF with 4 equiv of *N*-methylimidazole (*N*-MeIm) at room temperature to form a dark green solution from which divalent $SmI_2(N\text{-MeIm})_4$ (**1**) can be isolated in 95% yield. Crystallization of **1** from THF occurs with loss of 1 equiv of *N*-MeIm per samarium to form the dimer $[SmI(\mu\text{-}I)(N\text{-MeIm})_3]_2$ (**2**). **2** forms in space group $P2_1/n$ (C_{2h}^5; No. 14) with unit cell parameters at 168 K of a = 12.8310(12) Å, b = 9.9430(8) Å, c = 16.1339(11) Å, β = 109.735(6)°, and V = 1937.4(3) Å^3 with Z = 2 for D_{calcd} = 2.23 g cm^{-3}. Least-squares refinement of the model based on 3887 observed reflections ($|F_o| > 3.0\sigma(|F_o|)$) converged to a final R_F = 4.7%. The two six-coordinate samarium centers in **2** are edge-fused octahedra with the two bridging iodides and the terminal iodide attached to each samarium in a meridional orientation. $EuI_2(THF)_2$ reacts similarly to form $EuI_2(N\text{-MeIm})_4$ (**3**), which crystallizes from THF as $[EuI(\mu\text{-}I)(N\text{-MeIm})_3]_2$ (**4**). **4** is isostructural with **2** with unit cell parameters at 173 K of a = 12.810(14) Å, b = 9.910(9) Å, c = 16.121(15) Å, β = 109.90(8)°, and V = 1923.8(33) Å^3 with Z = 2 for D_{calcd} = 2.25 g cm^{-3}. Crystallization of divalent **1** from *N*-MeIm by diffusion of benzene occurs slowly (7–10 days) and leads to the trivalent complexes $[Sm(N\text{-MeIm})_8]I_3$ (**5**) and $\{[(N\text{-MeIm})_4Sm(\mu\text{-}OH)]_3(\mu_3\text{-}OH)_2\}I_4$ (**6**), which are formed by hydrolysis. **5** can be independently synthesized in 95% yield by isolating the solid from the pale yellow solution formed by dissolving $SmI_3(THF)_3$ in *N*-MeIm. **5** crystallizes from *N*-MeIm/benzene in space group $P4$ (C_4^1; No. 75) with unit cell parameters at 163 K of a = 10.3743(9) Å, c = 12.377(2) Å, and V = 1332.0(3) Å^3 with Z = 1 for D_{calcd} = 1.676 g cm^{-3}. Least-squares refinement of the model based on 1537 observed reflections ($|F_o| > 6.0\sigma(|F_o|)$) converged to a final R_F = 3.1%. In **5**, eight *N*-MeIm ligands describe a square antiprismatic geometry around the Sm(III) cation, which is not within bonding distance of the three iodide counterions. **6** crystallizes from *N*-MeIm/benzene in space group $Pbca$ (D_{2h}^{15}; No. 61) with unit cell parameters at 163 K of a = 21.217(3) Å, b = 27.497(6) Å, c = 33.497(5) Å, and V = 19 543(6) Å^3 with Z = 8 for D_{calcd} = 1.673 g cm^{-3}. Least-squares refinement of the model based on 7546 observed reflections ($|F_o| > 4.0\sigma(|F_o|)$) converged to a final R_F = 6.5%. **6** is composed of a triangle of $Sm(N\text{-MeIm})_4$ units bridged by three μ-hydroxide ligands in the plane of the metals and two μ_3-hydroxides above and below the plane. The geometry around samarium is best described as a dodecahedron. The four iodide counterions do not interact with the samarium centers. **5** is also very soluble in *N*-MeIm, and crystallization over long time periods leads to a hydroxide complex $[(N\text{-MeIm})_5Sm(\mu\text{-}OH)]_2I_4$ (**7**). **7** crystallizes from *N*-MeIm/benzene in space group $C2/c$ (C_{2h}^6; No. 15) with unit cell parameters at 163 K of a = 21.673(3) Å, b = 12.582(2) Å, c = 24.534(4) Å, β = 103.515(12)°, and V = 6504(2) Å with Z = 4 for D_{calcd} = 1.778 g cm^{-3}. Least-squares refinement of the model based on 6022 observed reflections ($|F_o| > 3.0\sigma(|F_o|)$) converged to a final R_F = 3.8%. **7** is composed of a dimeric tetracation which contains seven-coordinate samarium centers. Two $Sm(N\text{-MeIm})_5$ units are bridged by two μ-hydroxide ligands. As in **5** and **6**, the iodide counterions do not interact with the samarium centers.

Introduction

Recent studies of metal chalcogenide chemistry showed that *N*-methylimidazole (*N*-MeIm) is a powerful donor solvent which can stabilize species difficult to isolate in other solvents.[1-6] We have explored the utility of *N*-MeIm in samarium chemistry by investigating the behavior of the simple samarium iodides $SmI_2(THF)_2$ and $SmI_3(THF)_3$ in this solvent.

Relatively little structural information is available on samarium iodides, despite the fact that $SmI_2(THF)_2$ is used extensively in organic synthesis.[7-9] We report here that the strong donor power of *N*-MeIm readily provides crystallographically characterizable samarium iodide complexes. Moreover, this solvent allows the isolation of a new series of polymetallic samarium complexes bridged by hydroxide ligands. Hydroxide ligands are of interest in yttrium and lanthanide chemistry as reaction sites for condensation to bridged oxides,[10,11] but the number of crystallographically characterized hydroxide complexes of these metals is not large.[13-22] The formation of some europium analogs of the samarium complexes is also described.

Experimental Section

The compounds described below were handled under nitrogen using Schlenk double-manifold, high-vacuum, and glovebox (Vacuum Atmo-

* Abstract published in *Advance ACS Abstracts*, June 1, 1994.

(1) Dev, S.; Ramli, E.; Rauchfuss, T. B.; Stern, C. L. *J. Am. Chem. Soc.* **1990**, *112*, 6385–6386.
(2) Dev, S.; Ramli, E.; Rauchfuss, T. B.; Wilson, S. R. *Inorg. Chem.* **1991**, *30*, 2514–2519.
(3) Ramli, E.; Rauchfuss, T. B.; Stern, C. L. *J. Am. Chem. Soc.* **1990**, *112*, 4043–4044.
(4) Rauchfuss, T. B.; Dev, S.; Wilson, S. R. *Inorg. Chem.* **1992**, *31*, 154–156.
(5) Wozniak, M. E.; Sen, A.; Rheingold, A. L. *Chem. Mater.* **1992**, *4*, 753–755.
(6) Sundberg, R. J.; Martin, R. B. *Chem. Rev.* **1974**, *74*, 471–517.
(7) Girard, P.; Namy, J. L.; Kagan, H. B. *J. Am .Chem. Soc.* **1980**, *102*, 2693–2698.
(8) Namy, J. L.; Kagan, H. B. In *Handbook on the Physics and Chemistry of Rare Earths*; Gschneidner, K. A., Jr., Eyring, L., Eds.; Elsevier: Amsterdam, 1984; Vol. 6, Chapter 50. Namy, J. L.; Kagan, H. B. *Tetrahedron* **1986**, *24*, 6573–6614.
(9) Molander, G. A *Chem. Rev.* **1992**, *92*, 29–68.
(10) Brown, L. M.; Mazdiyasni, K. S. *Inorg. Chem.* **1970**, *9*, 2783–2786.
(11) Hubert-Pfalzgraf, L. G. *New J. Chem.* **1987**, *11*, 663–675.
(12) Evans, W. J.; Sollberger, M. S. *Inorg. Chem.* **1988**, *27*, 4417–4423.

0020-1669/94/1333-3072$04.50/0

Table 1. Experimental X-ray Data for $[SmI(\mu\text{-}I)(N\text{-MeIm})]_2$ (**2**), $[EuI(\mu\text{-}I)(N\text{-MeIm})_3]_2$ (**4**), $[Sm(N\text{-MeIm})_8I_3$ (**5**), $\{[(N\text{-MeIm})_4Sm](\mu\text{-OH})]_3(\mu_3\text{-OH})_2\}I_4$ (**6**), and $[(N\text{-MeIm})_5Sm(\mu\text{-OH})]_2I_4$ (**7**)

	2	**4**	**5**	**6**	**7**
formula	$C_{24}H_{36}N_{12}I_4Sm_2$	$C_{24}H_{46}N_{12}I_4Eu_2$	$C_{32}H_{48}N_{16}I_3Sm\cdot 2C_6H_6$	$C_{48}H_{77}N_{24}O_5I_4Sm_3\cdot 2C_4H_6N_2\cdot 2.5C_6H_6\cdot C_4H_8O$	$C_{40}H_{56}N_{20}O_2Sm_2I_4\cdot C_6H_6$
fw	1300.9	1304.2	1344.1	2460.6	1741.5
temp (K)	168	163	163	163	163
space group	$P2_1/n$ (C_{2h}^5; No. 14)	$P2_1/n$ (C_{2h}^5; No. 14)	$P4$ (C_4^1; No. 75)	$Pbca$ (D_{2h}^{15}; No. 61)	$C2/c$ (C_{2h}^6; No. 15)
a (Å)	12.8310(12)	12.810(4)	10.3743(9)	21.217(3)	21.673(3)
b (Å)	9.9430(8)	9.910(9)		27.497(6)	12.582(2)
c (Å)	16.1339(11)	16.121(15)	12.377(2)	33.497(5)	24.534(4)
β (deg)	109.735(6)	109.90(8)			103.515(12)
V (Å^3)	1937.4(3)	1924(3)	1332.0(3)	19 543(6)	6504(3)
Z	2	2	1	8	4
ρ_{calc} (g/cm^3)	2.23	2.25	1.676	1.673	1.778
λ(Mo Kα) (Å)	0.710 73	0.710 73	0.710 73	0.710 73	0.710 73
μ (mm^{-1})	6.20	6.44	2.870	3.095	3.722
R_F (%)	4.7	7.4	3.1	6.5	3.8
R_{wF} (%)	5.1	8.5	3.8	6.8	4.4

[a] $R_F = 100[\sum||F_o| - |F_c||/\sum|F_o|]$; $R_{wF} = 100[\sum w(|F_o| - |F_c|)^2/\sum w|F_o|^2]$.

spheres HE-553 Dri-Lab) techniques. Solvents were dried and physical measurements were obtained as previously described.[23] $SmI_2(THF)_2$,[7] $EuI_2(THF)_2$,[24a] and $SmI_3(THF)_3$[24b] were prepared from the metal and 1,2-diiodoethane. Redistilled *N*-methylimidazole from Aldrich was used as received (water content determined to be 0.013% by the Analytische Laboratorien GmbH, D-51647 Gummersbach, Germany).

$SmI_2(N\text{-MeIm})_4$ (1) and $[SmI(\mu\text{-}I)(N\text{-MeIm})_3]_2$ (2). In the glovebox, addition of *N*-MeIm (0.30 mL, 3.65 mmol) to a solution of $SmI_2(THF)_2$ (500 mg, 0.91 mmol) in 50 mL of THF caused an immediate color change to dark green. After 20 min, the solvent was removed. The residue was washed with toluene to give **1** as a dark green powder (635 mg, 95%). Anal. Calcd for $C_{16}H_{24}N_8I_2Sm$: C, 26.23; H, 3.30; N, 15.30; I, 34.64; Sm, 20.53. Found: C, 26.00; H, 3.28; N, 15.13; I, 34.41; Sm, 20.45. ^{1}H NMR (C_4D_8O, 300 MHz, 25 °C): δ 3.05 (s, 3 H, CH_3), 5.06 (s, 1 H, CH), 5.78 (s, 1 H, CH), 6.04 (s, 1 H, CH). ^{13}C NMR (C_4D_8O, 300 MHz, 25 °C): δ 30.6 (CH_3), 113.4 (CH). IR (Nujol): 1656 w, 1625 w, 1531 s, 1513 s, 1425 s, 1281 s, 1231 vs, 1113 s, 1106 s, 1094 vs, 1075 s, 1025 m, 925 vs, 844 m, 831 vs, 775 m, 769 s, 756 s, 663 vs, 619 s cm^{-1}. The complex is soluble in *N*-MeIm and THF. Crystallization of **1** from hot THF gave dark green single crystals of **2**, which was identified by X-ray diffraction.

X-ray Data Collection, Structure Determination, and Refinement for $[SmI(\mu\text{-}I)(N\text{-MeIm})_3]_2$ (2). Under nitrogen, a dark green crystal of approximate dimensions 0.10 × 0.25 × 0.33 mm^3 was immersed in Paratone-D oil. The oil-coated crystal was then manipulated in air onto a glass fiber and transferred to the nitrogen stream of a Siemens $P2_1$ diffractometer equipped with a modified LT-1 low-temperature system. The determination of Laue symmetry, crystal class, unit cell parameters, and the crystal's orientation matrix were carried out by previously described methods similar to those of Churchill.[25] Intensity data were collected at 168 K using a θ–2θ scan technique with Mo Kα radiation under the conditions given in Table 1. All 4927 data were corrected for absorption and for Lorentz and polarization effects and were placed on an approximately absolute scale. The diffraction symmetry was $2/m$ with systematic absences $0k0$ for $k = 2n + 1$ and $h0l$ for $h + l = 2n + 1$. The centrosymmetric monoclinic space group $P2_1/n$, a nonstandard setting of $P2_1/c$ (C_{2h}^5; No. 14), is therefore uniquely defined.

All crystallographic calculations were carried out using either our locally modified version of the UCLA Crystallographic Computing Package[26] or the SHELXTL PLUS program set.[27] The analytical scattering factors for neutral atoms were used throughout the analysis; both the real ($\Delta f'$) and imaginary ($i\Delta f''$) components of anomalous dispersion were included.[28a] The quantity minimized during least-squares analysis was $\sum w(|F_o| - |F_c|)^2$ where $w^{-1} = \sigma^2(|F_o|) + 0.0002(|F_o|)^2$.

The structure was solved by direct methods (SHELXTL PLUS) and refined by full-matrix least-squares techniques. The molecule is a dimer which is located about an inversion center. Hydrogen atoms were included using a riding model with d(C–H) = 0.96 Å and U(iso) = 0.05 Å^2. Refinement of positional and thermal parameters led to convergence with $R_F = 4.7\%$, $R_{wF} = 5.1\%$, and GOF = 2.37 for 191 variables refined against those 3887 data with $|F_o| > 3.0\sigma(|F_o|)$. A final difference-Fourier synthesis yielded ρ(max) = 3.02 e Å^{-3} at a distance of 0.82 Å from Sm(1).

$EuI_2(N\text{-MeIm})_4$ (3) and $[EuI(\mu\text{-}I)(N\text{-MeIm})_3]_2$ (4). In the glovebox, addition of *N*-MeIm (0.30 mL, 3.65 mmol) to a solution of $EuI_2(THF)_2$ (500 mg, 0.91 mmol) in 50 mL of THF caused an immediate color change from golden to bright yellow. After 20 min, the solvent was removed. The residue was washed with toluene to give **3** as a yellow powder (635 mg, 95%). Anal. Calcd for $C_{16}H_{24}N_8I_2Eu$: C, 26.18; H, 3.29; N, 15.26; I, 34.57; Eu, 20.70. Found: C, 26.02; H, 3.40; N, 15.12; I, 34.70; Eu, 20.85. IR (Nujol): 1521 m, 1507 m, 1498 s, 1471 s, 1465 s, 1457 s, 1419 m, 1376 m, 1368 m, 1285 m, 1280 m, 1232 s, 1107 s, 1101 s, 1090 s, 1079 s, 1028 m, 925 vs, 846 m, 827 s, 771 m, 753 s, 725 w, 660 vs, 619 s cm^{-1}. The complex is soluble in *N*-MeIm and THF. Crystallization of **3** from hot THF gave **4** as yellow single crystals. **4** is isostructural with **2** and was fully characterized by X-ray diffraction.

X-ray Data Collection, Structure Determination, and Refinement for $[EuI(\mu\text{-}I)(N\text{-MeIm})_3]_2$ (4). Under nitrogen, a yellow crystal of approximate dimensions 0.15 × 0.24 × 0.30 mm was handled as described above for **2**. To determine if **4** was isostructural with **2**, a limited data set ($2\theta_{max} = 35.0°$) was collected via an ω scan technique on a Siemens R3m/V diffractometer system equipped with a modified LT-2 low-temperature system at 168 K using monochromatized Mo Kα radiation ($\lambda = 0.710\ 73$ Å). The coordinates of the samarium analogue were used as a starting model for least-squares refinement. The model refined to $R_F = 7.4\%$ for those 1101 data with $|F_o| > 3.0\sigma(|F_o|)$ (Table 1).

(13) Baraniak, E.; Bruce, R. St. L.; Freeman, H. C.; Hair, N. J.; James, J. *Inorg. Chem.* **1976**, *15*, 2226–2230.
(14) Rebizant, J.; Spirlet, M. R.; Barthélemy, P. P.; Desreux, J. F. *J. Inclusion Phenom.* **1987**, *5*, 505–513.
(15) Bukietyńska, K.; Pham, N. T.; Starynowicz, P. *Acta Crystallogr.* **1989**, *C45*, 553–556.
(16) Evans, W. J.; Hozbor, M. A.; Bott, S. G.; Atwood, J. L. *Inorg. Chem.* **1988**, *27*, 1990–1993.
(17) Toledano, P.; Ribot, F.; Sanchez, C. *C. R. Acad. Sci. Paris* **1990**, *311*, 1315–1320.
(18) (a) Hitchcock, P. B.; Lappert, M. F.; Prashar, S. *J. Organomet. Chem.* **1991**, *413*, 79–90. (b) Beletskaya, I. P.; Voskoboynikov, A. Z.; Chuklanova, E. B.; Kirillova, N. I.; Shestakova, A. K.; Parshina, I. N.; Gusev, A. I.; Magomedov, G. K.-I. *J. Am. Chem. Soc.* **1993**, *115*, 3156–3166.
(19) Schumann, H.; Loebel, J.; Pickardt, J.; Qian, C.; Xie, Z. *Organometallics* **1991**, *10*, 215–219. Schumann, H.; Görlitz, F. H.; Hahn, F. E.; Pickardt, J.; Qian, C.; Xie, Z. *Z. Anorg. Allg. Chem.* **1992**, *609*, 131–138.
(20) Deacon, A. B.; Feng, T.; Nickel, S.; Ogden, M. I.; White, A. H. *Aust. J. Chem.* **1992**, *45*, 671–683.
(21) Hermann, W. A.; Anwander, R.; Kleine, M.; Öfele, K.; Riede, J.; Scherer, W. *Chem. Ber.* **1992**, *125*, 2391–2397
(22) Deng, D.; Song, F.; Wang, Z.; Qian, C.; Wu, G.; Zheng, P. *Polyhedron* **1992**, *11*, 2883–2887.
(23) Evans, W. J.; Chamberlain, L. R.; Ulibarri, T. A.; Ziller, J. W. *J. Am. Chem. Soc.* **1988**, *110*, 6423–6432.
(24) (a) Watson, P. L.; Tulip, T. H.; Williams, I. *Organometallics* **1990**, *9*, 1999–2009. (b) Deacon, G. B.; Koplick, A. J. *Inorg. Nucl. Chem. Lett.* **1979**, *15*, 263–265.
(25) Churchill, M. R.; Lashewycz, R. A.; Rotella, F. J. *Inorg. Chem.* **1977**, *16*, 265–271.
(26) *UCLA Crystallographic Computing Package*; University of California: Los Angeles, CA, 1981. Strouse, C. Personal communication.
(27) Sheldrick, G. M. *SHELXTL PLUS*; Siemens Analytical X-ray Instruments, Inc.; Madison, WI, 1990.
(28) (a) *International Tables for X-ray Crystallography*; Kluwer: Dordrecht, The Netherlands, 1992; Vol. C. (b) Rogers, D. *Acta Crystallogr.* **1981**, *A37*, 734–741.

$[Sm(N\text{-MeIm})_8]I_3$ (5) and $\{[(N\text{-MeIm})_4Sm(\mu\text{-OH})]_3(\mu_3\text{-OH})_2\}I_4$ (6). Diffusion of benzene into a solution of **1** in *N*-MeIm in the glovebox requires 7–10 days to form crystals, and this reproducibly gives a mixture of two types of THF-insoluble crystals which were separated by hand and characterized by X-ray crystallography. The pale yellow crystals were identified as **5**, and the colorless crystals were **6**. Analytical data were not obtained on the mixture of crystals, but data on a desolvated analog of **6** were collected as follows. Attempts to crystallize **1** from THF at ambient temperature in the glovebox led over a period of 2 days to a slow formation of a THF-insoluble colorless material whose elemental analysis matches that of **6** less one *N*-MeIm per samarium: Anal. Calcd for $C_{36}H_{59}N_{18}O_5I_4Sm_3$: C, 24.25; H, 3.34; N, 14.14; I, 28.47; Sm, 25.31. Found: C, 24.43; H, 3.21; N, 14.07; I, 28.71; Sm, 24.95.

$[Sm(N\text{-MeIm})_8]I_3$ (5). In the glovebox, $SmI_3(THF)_3$ (500 mg, 0.66 mmol) was dissolved in 10 mL of *N*-MeIm. The color changed slowly from yellow to pale yellow. After 20 min, the solvent was removed under high vacuum (10^{-5} Torr). The residue was washed with THF to give **5** as a pale bronze powder (755 mg, 95%). Anal. Calcd for $C_{32}H_{48}N_{16}I_3Sm$: C, 32.35; H, 4.07; N, 18.87; I, 32.05; Sm, 12.66. Found: C, 32.48; H, 4.19; N, 18.72; I, 31.98; Sm, 12.45. IR (Nujol): 1653 w, 1537 m, 1534 m, 1516 m, 1508 m, 1425 m, 1419 m, 1286 m, 1228 s, 1083 s, 1028 w, 932 s, 830 m, 757 s, 743 s, 669 s, 662 s, 603 vs cm^{-1}. The THF-insoluble complex is soluble in *N*-MeIm. Crystals of **5** were obtained as described above and fully characterized by X-ray diffraction.

X-ray Data Collection, Structure Determination, and Refinement for $[Sm(N\text{-MeIm})_8]I_3$ (5). Under nitrogen, a pale bronze crystal of approximate dimensions $0.20 \times 0.23 \times 0.33$ mm^3 was handled as described above for **2**, and intensity data were collected as described for **2** at 163 K. Details appear in Table 1.

All 1790 data were corrected for absorption and for Lorentz and polarization effects and placed on an approximately absolute scale. Any reflection with I(net) < 0 was assigned the value $|F_o| = 0$. The crystal system is tetragonal, and there are no systematic absences. The space group was later determined to be the noncentrosymmetric $P4$ (C_4^1; No. 75) by successful refinement of the model. All crystallographic calculations were carried out as desribed above for **2**. The quantity minimized during least-squares analysis was $\sum w(|F_o| - |F_c|)^2$ where $w^{-1} = \sigma^2(|F_o|) + 0.0002(|F_o|)^2$.

The structure was solved by direct methods (SHELXTL PLUS) and refined by full-matrix least-squares techniques. The molecule is located on a site of 4-fold symmetry at (0, 0, 0). Sm(1) has a site-occupancy-factor of $^1/_4$. I(1) is located on a 2-fold axis parallel to z at $x = {}^1/_2$ and $y = 0$ with a SOF = 0.50 and I(2) is on a 4-fold axis parallel to z at $x = {}^1/_2$ and $y = {}^1/_2$ with SOF = 0.25. The site symmetry associated with these three atoms is consistent with the 3:1 (I:Sm) ratio for the Sm(III) complex. There are two benzene molecules present in the asymmetric unit. Each is disordered and located about a site of 4-fold symmetry. Two carbon atoms (SOF = 0.75) define the eight disordered components of each ring. Hydrogen atoms were included using a riding model with d(C–H) = 0.96 Å and U(iso) = 0.08 Å^2. The hydrogen atoms associated with the disordered benzene molecules were not included in the refinement. Refinement of the model led to convergence with $R_F = 3.1\%$, $R_{wF} = 3.8\%$, and GOF = 1.73 for 137 variables refined against those 1537 data with $|F_o| > 6.0\sigma(|F_o|)$. A final difference-Fourier map was "clean", ρ(max) = 1.04 e Å^{-3}. The absolute structure was determined from the diffraction experiment by refinement of Roger's η parameter[28b] ($\eta = 1.29(11)$).

X-ray Data Collection, Structure Determination, and Refinement for $\{[(N\text{-MeIm})_4Sm(\mu\text{-OH})]_3(\mu_3\text{-OH})_2\}I_4$ (6). Under nitrogen, a colorless crystal of approximate dimensions $0.33 \times 0.35 \times 0.37$ mm^3 was handled as described above for **2**. Intensity data were collected at 163 K. Details appear in Table 1.

All 13 849 data were corrected for absorption and for Lorentz and polarization effects and placed on an approximately absolute scale. A careful examination of a preliminary data set revealed the systematic extinctions $0kl$ for $k = 2n + 1$, $h0l$ for $h = 2n + 1$, and $hk0$ for $h = 2n + 1$. The centrosymmetric orthorhombic space group $Pbca$ (D_{2h}^{15}; No. 61) is therefore uniquely defined. All crystallographic calculations were carried out as described above for **2**. The quantity minimized during least-squares analysis was $\sum w(|F_o| - |F_c|)^2$ where $w^{-1} = \sigma^2(|F_o|) + 0.0006(|F_o|)^2$.

The structure was solved by direct methods (SHELXTL PLUS) and refined by full-matrix least-squares techniques. There are two molecules of *N*-MeIm, 2.5 molecules of benzene, and a molecule of THF present in the asymmetric unit. The benzene molecule defined by atoms C(49), C(50), and C(51) is located on a center of inversion at (0, 0, $^1/_2$). The benzene ring (C(70)–C(75)) was refined as a regular hexagon (d(C–C) = 1.395 Å) without hydrogens. The remaining hydrogen atoms were included using a riding model with d(C–H) = 0.96 Å, d(O–H) = 0.85 Å, and U(iso) = 0.08 Å^2. Refinement of positional and thermal parameters led to convergence with $R_F = 6.5\%$, $R_{wF} = 6.8\%$, and GOF = 1.54 for 868 variables refined against those 7546 data with $|F_o| > 4.0\sigma(|F_o|)$. A final difference-Fourier map was featureless, ρ(max) = 1.34 e Å^{-3}.

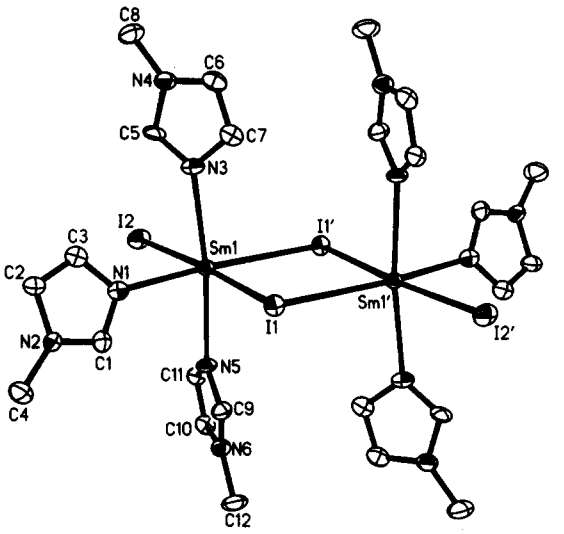

Figure 1. Thermal ellipsoid plot of $[SmI(\mu\text{-I})(N\text{-MeIm})_3]_2$ (**2**), drawn at the 50% probability level.

X-ray Data Collection, Structure Determination, and Refinement for $[(N\text{-MeIm})_5Sm(\mu\text{-OH})]_2I_4$ (7). Diffusion of benzene into a solution of **5** in *N*-MeIm in the glovebox over 2 months gave THF-insoluble colorless crystals of **7**. Under nitrogen, a colorless crystal of approximate dimensions $0.30 \times 0.40 \times 0.46$ mm^3 was handled as described above for **2**. Intensity data were collected at 163 K. Details appear in Table 1.

All 8073 data were corrected for absorption and for Lorentz and polarization effects, merged to yield a unique data set, and placed on an approximately absolute scale. Any reflection with I(net) < 0 was assigned the value $|F_o| = 0$. The systematic extinctions observed were hkl for $h + k = 2n + 1$ and $h0l$ for $l = 2n + 1$; the diffraction symmetry was $2/m$. The two possible monoclinic space groups are Cc (C_s^4; No. 9) and $C2/c$ (C_{2h}^6; No. 15). The centrosymmetric space was chosen and later shown to be the correct choice. All crystallographic calculations were carried out as described above for **2**. The quantity minimized during least-squares analysis was $\sum w(|F_o| - |F_c|)^2$ where $w^{-1} = \sigma^2(|F_o|) + 0.0003(|F_o|)^2$.

The structure was solved by direct methods (SHELXTL PLUS) and refined by full-matrix least-squares techniques. The dimeric molecule is located about a 2-fold rotation axis. There is a benzene solvent molecule also located about a 2-fold axis. There are no atoms located on special positions; therefore, all site occupancy factors are 1.0. Hydrogen atoms were included using a riding model with d(C–H) = 0.96 Å and U(iso) = 0.08 Å^2. The hydroxide hydrogen atom H(1) was located from a difference map. It was included with fixed (x, y, z) and U(iso) = 0.08 Å^2 (d(O–H) = 1.11 Å). Refinement of positional and anisotropic thermal parameters led to convergence with $R_F = 3.8\%$, $R_{wF} = 4.4\%$, and GOF = 1.54 for 334 variables refined against those 6022 data with $|F_o| > 3.0\sigma(|F_o|)$. A final difference-Fourier map was devoid of significant features, ρ(max) = 0.95 e Å^{-3}.

Results

A Divalent Bimetallic Complex: $[SmI(\mu\text{-I})(N\text{-MeIm})_3]_2$ (2). Dark blue $SmI_2(THF)_2$ reacts in THF with 4 equiv of *N*-MeIm to form a dark green solution. Removal of solvent leaves a dark green material which analyzes as $SmI_2(N\text{-MeIm})_4$ (**1**). Attempts to crystallize **1** from *N*-MeIm by benzene diffusion require long time periods and lead to the trivalent hydrolysis products described below. However, crystallization of **1** from hot THF forms crystals of divalent $[SmI(\mu\text{-I})(N\text{-MeIm})_3]_2$, **2**, the structure of which is shown in Figure 1.

"SmI_2/N-MeIm" crystallizes as a dimer in which each samarium atom exhibits an octahedral coordination environment composed of one terminal and two bridging iodide ligands and three terminal *N*-MeIm ligands. The three (ligand)–Sm–(trans

Table 2. Selected Bond Distances (Å) and Angles (deg) for $[SmI(\mu\text{-}I)(N\text{-}MeIm)_3]_2$ (**2**) and $[Sm(N\text{-}MeIm)_8]I_3$ (**5**)

2		**5**	
Sm(1)–N(1)	2.621(7)	Sm(1)–N(1)	2.563(6)
Sm(1)–N(3)	2.641(6)	Sm(1)–N(3)	2.596(6)
Sm(1)–N(5)	2.639(6)		
Sm(1)–I(1)	3.280(1)		
Sm(1)–I(2)	3.237(1)		
Sm(1′)–I(1)	3.307(1)		
I(1)–Sm(1)–I(2)	175.7(1)		
I(1)–Sm(1)–I(1′)	84.0(1)		
I(2)–Sm(1)–I(1′)	100.2(1)		
Sm(1)–I(1)–Sm(1′)	96.0(1)		
N(1)–Sm(1)–N(3)	86.5(2)	N(1)–Sm(1)–N(3)	75.5(2)
N(1)–Sm(1)–N(5)	88.4(1)	N(1)–Sm(1)–N(1a)	115.5(3)
N(3)–Sm(1)–N(5)	173.2(2)	N(3)–Sm(1)–N(1a)	145.3(2)
I(1)–Sm(1)–N(1)	84.4(1)	N(1)–Sm(1)–N(1b)	73.5(1)
I(2)–Sm(1)–N(1)	91.5(1)	N(3)–Sm(1)–N(1b)	139.2(2)
I(1)–Sm(1)–N(3)	94.2(1)	N(3)–Sm(1)–N(1c)	79.3(2)
I(2)–Sm(1)–N(3)	86.8(1)	N(3)–Sm(1)–N(3a)	115.1(3)
I(1)–Sm(1)–N(5)	88.4(1)		
I(2)–Sm(1)–N(5)	90.0(1)		
N(1)–Sm(1)–I(1′)	168.3(1)		
N(3)–Sm(1)–I(1′)	93.4(2)		
N(5)–Sm(1)–I(1′)	93.1(2)		

ligand) angles are 175.7(1), 173.2(2), and 168.3(1)°, and the (ligand)–Sm–(cis ligand) angles vary from 84.0(1) to 96.0(1)° (Table 2). The three iodide ligands around each samarium have a meridional orientation. The overall structure is similar to that recently reported for $[YbCl_3(THF)_2]_2$ except that the halide and solvate ligands have been interchanged.[29]

Bond distances in **2** can be compared to those of the structures of three other iodide-bridged Sm(II) complexes, $[Sm(\mu\text{-}I)_2(NCCMe_3)_2]_n$ (**8**),[30] $[(C_5Me_5)Sm(\mu\text{-}I)(THF)_2]_2$ (**9**),[31] and $\{[(Me_3Si)_2N]Sm(\mu\text{-}I)(THF)(DME)\}_2$ (**10**).[32] **2** is structurally most similar to **8** in that both are diiodides which contain six-coordinate samarium centers. The main difference in these two complexes is that all of the iodides in **8** are bridged to give a polymer, whereas only half of the iodides in **2** bridge to generate a dimer. The bridging 3.280(1) and 3.307(1) Å Sm–I bonds in **2** are intermediate in length compared to the analogous distances in **8**, 3.242(1) Å, **9**, 3.356(2) and 3.459(2) Å, and **10**, 3.3414(9) and 3.3553(9) Å. The 3.237(1) Å terminal Sm–I distance is shorter than the bridging distances in **2**, as is typical for terminal versus bridging ligands, but it is interesting to note that this terminal distance is equivalent to the bridging distance in **8**. The terminal Sm–I distance in **2** is also shorter than the 3.332(1) and 3.265(1) Å terminal Sm–I distances in eight-coordinate *cis*- and *trans*-$SmI_2[O(CH_2CH_2OMe)_2]_2$ (**11**[33] and **12**),[30] as is typical for lanthanides with different coordination numbers. The 0.16 Å difference between the terminal Sm–I distance in **2** and the 3.077(1) Å Sm–I distance in six-coordinate $[SmI_2(OPMePh_2)_4]I$ (**13**)[34] is also similar to differences previously observed in analogous Sm(II) and Sm(III) complexes.[35-37]

The 2.621(7)–2.641(6) Å Sm–N bonds in **2** are equivalent within the error limits to the 2.596(8) Å Sm–N($NCCMe_3$) bonds in **8**. Considering the difference in hybridization of the nitrogen atoms, this implies a stronger interaction in **2**. The fact that **2** crystallizes as a trisolvated dimeric species instead of a disolvated polymeric species as in **8** is also consistent with this. It is interesting to note that the three iodides and the three imidazoles in **2** are arranged in a meridional fashion. This decreases the number of trans (*N*-MeIm)–Sm–I linkages. In contrast, in **8** the two *tert*-butyl cyanide ligands adopt a cis configuration which leads to trans N–Sm–I linkages instead of trans N–Sm–N arrangements.

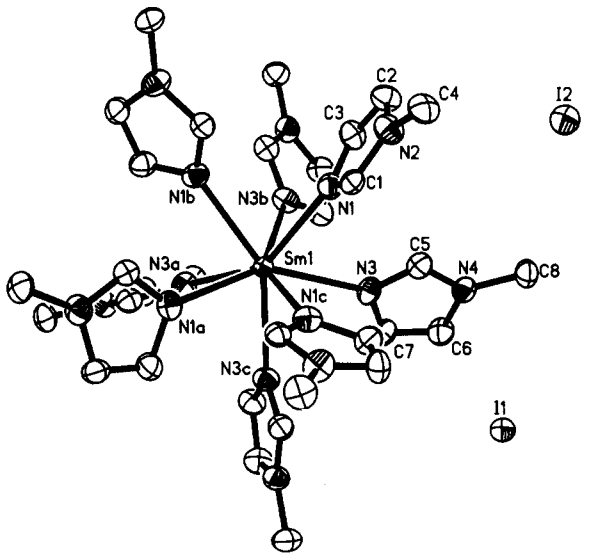

Figure 2. Thermal ellipsoid plot of $[Sm(N\text{-}MeIm)_8]I_3$ (**5**), drawn at the 50% probability level. Sm(1) has a site occupancy factor (SOF) of $^1/_4$. I(1) is located on a 2-fold axis at ($-^1/_2$, 0, *z*; SOF = $^1/_2$), and I(2) is on a 4-fold axis at ($-^1/_2$, $-^1/_2$, *z*; SOF = $^1/_4$). The site symmetry associated with these three atoms gives the 3:1 (I:Sm) ratio.

Europium Analogs of 1 and 2. Products analogous to **1** and **2** are formed when $EuI_2(THF)_2$ is reacted with 4 equiv of *N*-MeIm in THF. Yellow $EuI_2(N\text{-}MeIm)_4$ (**3**) can be isolated in 95% yield. Crystallization of **3** from hot THF leads to loss of 1 equiv of *N*-MeIm per europium to form $[EuI(\mu\text{-}I)(N\text{-}MeIm)_3]_2$ (**4**), which is isostructural with **2**.

A Monometallic Trivalent *N*-MeIm Octasolvate: $[Sm(N\text{-}MeIm)_8]I_3$ (5). **1** is sufficiently soluble in *N*-MeIm that direct crystallization from this solvent is slow. Invariably over long time periods, hydrolyzed and oxidized products were obtained when crystallization was attempted in *N*-MeIm. Under these conditions, two trivalent complexes are formed: a pale yellow product, **5**, and a colorless product, **6**, both of which have been identified by X-ray crystallography. Hydrogen was identified mass spectrometrically as a byproduct of this process.

The yellow product was shown to be $[Sm(N\text{-}MeIm)_8]I_3$ (**5**) (Figure 2). This complex can be independently synthesized in high yield by dissolving yellow $SmI_3(THF)_3$ in *N*-MeIm. A pale yellow solution forms, from which analytically pure $[Sm(N\text{-}MeIm)_8]I_3$ can be isolated.

Complex **5** contains an octasolvated samarium center in which the *N*-MeIm ligands have completely displaced the iodide counterions. The closest Sm···I distance is 7.42 Å. Among eight-coordinate complexes, relatively few are known which contain all unidentate ligands[38-42] as is found in **5**.

The eight nitrogen donor atoms in **5** describe a square antiprism as shown in Figure 3. The regularity of this geometry can be evaluated by examining the angle α, between the eight metal donor atom vectors and the 8-fold inversion axis which passes

(29) Deacon, G. B.; Feng, T.; Nickel, S.; Skelton, B. W.; White, A. H. *J. Chem. Soc., Chem. Commun.* **1993**, 1328–1329.
(30) Chebolu, V.; Whittle, R. R.; Sen, A. *Inorg. Chem.* **1985**, *24*, 3082–3085.
(31) Evans, W. J.; Grate, J. W.; Choi, H. W.; Bloom, I.; Hunter, W. E.; Atwood, J. L. *J. Am. Chem. Soc.* **1985**, *107*, 941–946.
(32) Evans, W. J.; Drummond, D. K.; Zhang, H.; Atwood, J. L. *Inorg. Chem.* **1988**, *27*, 575–579.
(33) Sen, A.; Chebolu, V.; Rheingold, A. L. *Inorg. Chem.* **1987**, *26*, 1821–1823.
(34) Sen, A.; Chebolu, V.; Holt, E. M. *Inorg. Chim. Acta* **1986**, *118*, 87–90.
(35) Evans, W. J.; Ulibarri, T. A.; Chamberlain, L. R.; Ziller, J. W.; Alvarez, D. *Organometallics* **1990**, *9*, 2124–2130.
(36) Shannon, R. D. *Acta Crystallogr.* **1976**, *A32*, 751–767.
(37) Evans, W. J.; Foster, S. E. *J. Organomet. Chem.* **1992**, *433*, 79–94.
(38) Al-Karaghouli, A. R.; Wood, J. S. *Inorg. Chem.* **1979**, *18*, 1177–1184.
(39) Castellini Bisi, C.; Della Giusta, A.; Coda, A.; Tuzzoli, V. *Cryst. Struct. Commun.* **1974**, *3*, 381.
(40) Fantin, C. A.; Zinner, L. B.; Vicentini, G.; Rodellas, C.; Niinisto, L. *Acta Chem. Scand.* **1987**, *A41*, 259–268.
(41) Mautner, F. A.; Krischner, H. *Monatsh. Chem.* **1990**, *121*, 781–786.
(42) Matsumura, N.; Takeuchi, T.; Ouchi, A. *Bull. Chem. Soc. Jpn.* **1990**, *63*, 620–622.

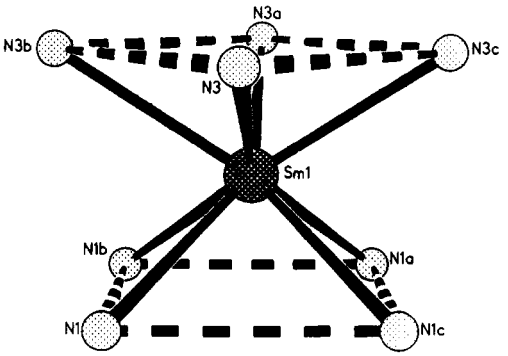

Figure 3. Geometry of the eight nitrogen donor atoms around samarium in $[Sm(N\text{-MeIm})_8]I_3$ (**5**).

through the metal in a regular square antiprism.[43] In the ideal case, α is 59.26°. In **5**, there are only two unique values of α, since there are only two crystallographically unique *N*-MeIm positions (involving N(1) and N(3)), and they are 57.8 and 57.6°, respectively.

The metrical data for trivalent **5** (Table 2) provide an interesting comparison with those for **2**. Although Sm(III) is smaller than Sm(II), which would lead to smaller distances in **5**,[35-37] **5** contains a higher coordinate samarium center than **2**, which could lead to longer distances.[36] These conflicting trends lead to distances that are rather similar: the two unique Sm–N distances in **5** are 2.563(6) and 2.596(6) Å, compared to the 2.621(7)–2.641(6) Å range of Sm–N distances found for **2**. On the basis of Shannon radii,[36] eight-coordinate Sm(III) is expected to be 0.07–0.10 Å smaller than six-coordinate Sm(II). The extremes of the Sm–N distances in the two complexes match this prediction.

The difference in coordination environments selected upon crystallization of **2** and **5** is also interesting. Although Sm(II) is larger than Sm(III), the samarium centers in **2** are six-coordinate rather than eight-coordinate as found in **5**. Although Sm(II) has a lower charge to radius ratio than Sm(III), it coordinates the anionic iodide ligands whereas this is not the case in **5**. However, since Sm(II) should be softer than Sm(III), one might expect a preference for the soft iodide ligands over the harder *N*-MeIm donor atoms. The fact that divalent **1** lost an *N*-MeIm ligand when **2** crystallized from solution is also consistent with this. Comparison of the space-filling models of **2** and **5** (Figure 4) shows how the *N*-MeIm ligands can accommodate different ligand sets to fill the coordination sphere of the metal.

A Trivalent Trimetallic Complex: $\{[(N\text{-MeIm})_4Sm(\mu\text{-OH})]_3(\mu_3\text{-OH})_2\}I_4$ (6). The other trivalent product isolated from the recrystallization of **1** from *N*-MeIm is the trimetallic hydroxo species $\{[(N\text{-MeIm})_4Sm(\mu\text{-OH})]_3(\mu_3\text{-OH})_2\}I_4$ (**6**), whose structure is shown in Figure 5. The structure of **6** is reminiscent of a large number of recently characterized yttrium and lanthanide alkoxide complexes of general formula $Ln_3(OR)_3(\mu\text{-OR})_3(\mu_3\text{-OR})(\mu_3\text{-Z})Z(L)_2$ (Ln = Y or a lanthanide; R = CMe_3; Z = OR, O, or a halide; L = THF or ROH).[44-48] The significant difference in **6** is that the bridging ligands are exclusively hydroxides and the terminal ligands are exclusively *N*-MeIm. Although several hydroxide complexes of the lanthanides have been structurally characterized, including $[Yb(C_5H_4NCH{=}NNHC_5H_4N)(H_2O)_3(\mu\text{-OH})]_2Cl_4\cdot 4H_2O$,[13] $[Pr_2(C_{16}H_{32}N_2O_5)_2(\mu\text{-OH})_2](ClO_4)_4\cdot 2CH_3CN$,[14] $[Ho_2(\mu\text{-OH})_2(C_{12}H_8N_2)_4(H_2O)_4](ClO_4)_4\cdot 2C_{12}H_8N_2$,[15] $[(C_5H_5)_2Y(\mu\text{-OH})]_2(C_6H_5C{\equiv}CC_6H_5)$,[16] $[Ce_6(\mu_3\text{-O})_4(\mu_3\text{-OH})_4(acac)_{12}]$,[17] $\{[C_5H_3(SiMe_3)_2]_2Ln(\mu\text{-OH})\}_2$ (Ln = Sm,[18a] Lu[18b]), $\{[C_5H_4(SiMe_3)]_2Yb(\mu\text{-OH})\}_2$,[18a] $[O(CH_2CH_2C_5H_4)_2Ln]_2(\mu\text{-OH})(\mu\text{-}N_2C_3HMe_2)$ (Ln = Y, Lu),[19] $[Yb(OC_6H_2{}^tBu_3\text{-}2,4,6)_2(\mu\text{-OH})(THF)]_2$,[20] $[(Me_3CC_5H_4)_2Ln(\mu\text{-OH})]_2$ (Ln = Nd, Dy),[21] $[(CH_3OCH_2CH_2C_5H_4)_2Er(\mu\text{-OH})]_2$,[22] and $[O(CH_2CH_2C_5H_4)_2Y(\mu\text{-OH})_2]$,[19] complex **6** is the first crystallographically characterized lanthanide complex in which all of the anionic ligands attached to the metals are hydroxides.

In contrast to the trimetallic $Ln_3(OR)_7Z_2(L)_2$ alkoxide complexes which contain six-coordinate metal centers, each samarium in **6** is eight-coordinate due to interaction with four terminal *N*-MeIm ligands and four bridging hydroxides (Figure 6). In contrast to the square antiprism in **5**, the eight donor atoms in **6** describe a dodecahedron. The bridging nature of the hydroxide ligands and their fixed location in the polymetallic skeleton constrain them to be on one side of the dodecahedron. Hence, the four hydroxide ligands occupy two of the four-coordinate sites and two of the five-coordinate sites present in a triangulated dodecahedron.

The Sm–N distances in **6** range from 2.538(16) to 2.631(12) Å (Table 3), a range which overlaps the two distinct Sm–N(*N*-MeIm) distances in eight-coordinate **5**. Comparison of the 2.323(11)–2.358(10) Å Sm–O(μ-OH) distances in **6** with the 2.40(2) and 2.41(1) Å doubly bridging hydroxide distances in $\{[C_5H_3(SiMe_3)_2]_2Sm(\mu\text{-OH})\}_2$[18a] suggests that they are normal. The 2.412(10)–2.465(9) Å Sm–O(μ_3-OH) distances are longer, as expected for triply bridging versus doubly bridging ligands. As in **5**, the iodide ligands are not attached to the samarium centers. The nonbonding Sm···I distances range from 5.998 to 8.539 Å.

A Trivalent Bimetallic Complex: $[(N\text{-MeIm})_5Sm(\mu\text{-OH})]_2I_4$ (7). Like divalent **1**, the trivalent complex $[Sm(N\text{-MeIm})_8]I_3$ (**5**) also hydrolyses over long periods of time in *N*-MeIm. Crystals of $[(N\text{-MeIm})_5Sm(\mu\text{-OH})]_2I_4$ (**7**) have been identified from this reaction, and the structure is shown in Figure 7. Unlike **5** and **6**, this trivalent samarium iodide forms a seven-coordinate complex. The coordination geometry around each samarium center can be viewed as a square-face-capped trigonal prism in which N(9) is the cap. The dimer is formed by edge sharing of the O(1)–O(1′) edge of the trigonal prism of each half of the molecule. As in **4**, all of the terminal ligands are *N*-MeIm and all of the bridging ligands are hydroxides. As in **5** and **6**, the iodide ligands again function only as noncoordinating counteranions. The Sm···I distances range from 5.18 to 6.34 Å.

The 2.504(4)–2.591(4) Å range of Sm–N distances (Table 3) overlaps the low end of the range of Sm–N(*N*-MeIm) distances in **5** and **6**, but the 2.544(8) Å average is less, as expected for a seven-coordinate complex, in comparison to the 2.580(17) Å average for eight-coordinate **5**. The 2.287(3) and 2.309(3) Å Sm–O(μ-OH) distances are also shorter than the 2.342(11) Å average found in **6**.

Discussion

N-Methylimidazole is a strong donor ligand for samarium complexes just as it is for other metal complexes.[1-6] It is very effective in dissolving both Sm(II) and Sm(III) complexes, and in the case of SmI_3, it is strong enough to completely displace all three anionic ligands and form the octasolvated trication $[Sm(N\text{-MeIm})_8]^{3+}$ found in **3**. Complete substitution of anionic ligands by *N*-MeIm has been observed before with iron,[49] cobalt,[50]

(43) Hoard, J. L.; Silverton, J. V. *Inorg. Chem.* **1963**, *2*, 235–243. Lippard, S. J. *Prog. Inorg. Chem.* **1967**, *8*, 109–157. Muetterties, E. L.; Wright, C. M. *Q. Rev. Chem. Soc.* **1967**, *21*, 109–194. Kepert, D. L. *Prog. Inorg. Chem.* **1985**, *24*, 179–249.
(44) Evans, W. J.; Sollberger, M. S.; Hanusa, T. P. *J. Am. Chem. Soc.* **1988**, *110*, 1841–1850.
(45) Bradley, D. C.; Chudzynska, H.; Hursthouse, M. B.; Motevalli, M. *Polyhedron* **1991**, *10*, 1049–1059.
(46) Evans, W. J.; Olofson, J. M.; Ziller, J. W. *J. Am. Chem. Soc.* **1990**, *112*, 2308–2314.
(47) Andersen, R. A.; Templeton, D. H.; Zalkin, A. *Inorg. Chem.* **1978**, *17*, 1962–1964.
(48) Evans, W. J.; Sollberger, M. S.; Khan, S. I.; Bau, R. *J. Am. Chem. Soc.* **1988**, *110*, 439–446.
(49) Miller, L. L.; Jacobson, R. A.; Chen, Y.-S.; Kurtz, D. M., Jr. *Acta Crystallogr.* **1989**, *C45*, 527–529.
(50) Marzotto, A.; Bianchi, A.; Valle G.; Clemente, D. A. *Acta Crystallogr.* **1989**, *C45*, 582–585.

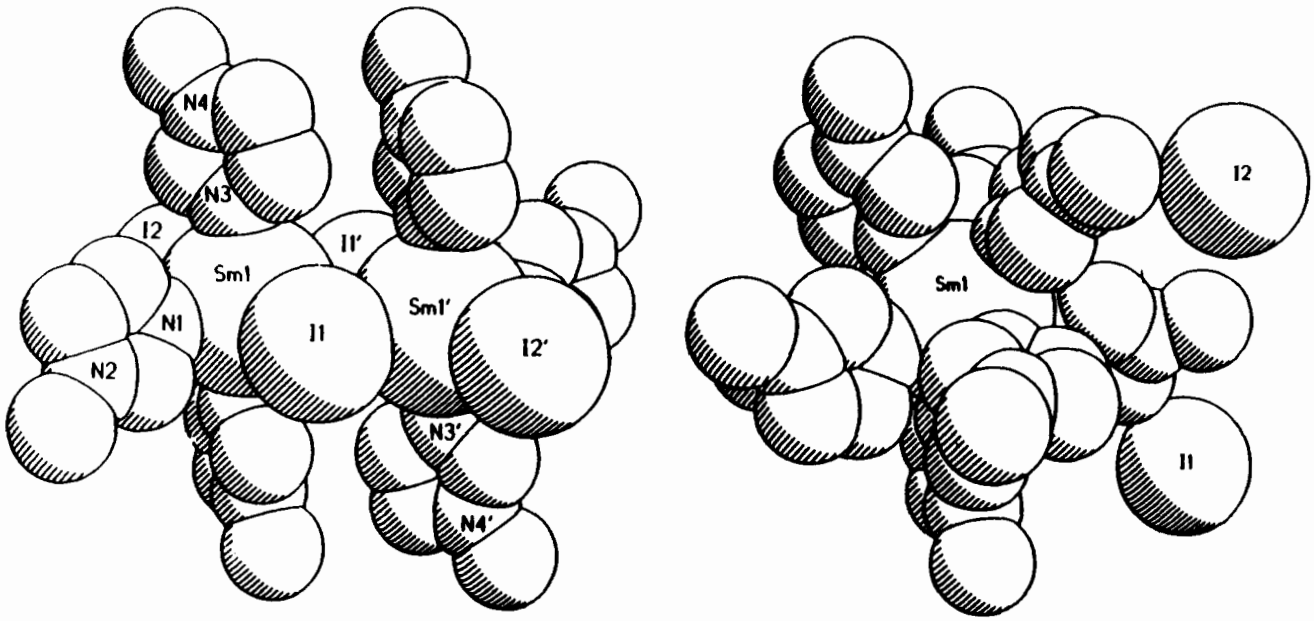

Figure 4. Space-filling models of $[SmI(\mu\text{-}I)(N\text{-}MeIm)_3]_2$ (**2**) (left) and $[Sm(N\text{-}MeIm)_8]I_3$ (**5**) (right).

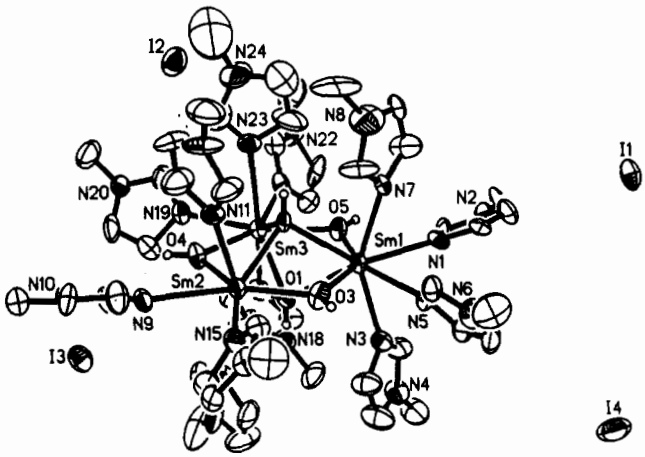

Figure 5. Thermal ellipsoid plot of $\{[(N\text{-}MeIm)_4Sm(\mu\text{-}OH)]_3(\mu_3\text{-}OH)_2\}I_4$ (**6**), drawn at the 50% probability level.

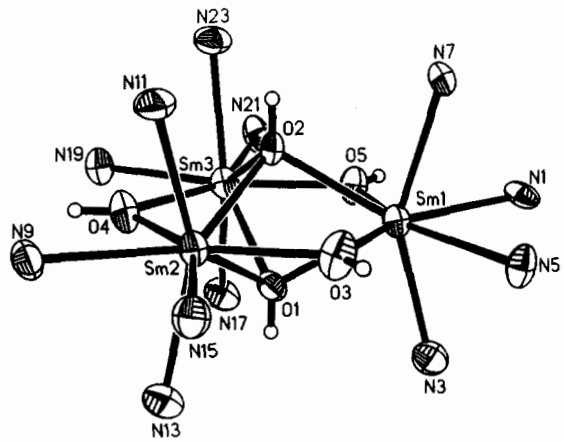

Figure 6. Thermal ellipsoid plot of the nitrogen and oxygen donor atoms around the samarium cations in $\{[(N\text{-}MeIm)_4Sm(\mu\text{-}OH)]_3(\mu_3\text{-}OH)_2\}I_4$ (**6**). The two trapezoids which define the dodecahedron around Sm(1) are O(5), N(1), N(5), O(3) and N(3), O(1), O(2), N(7).

nickel,[2] and copper[51] complexes, but crystallographic studies of lanthanide halide complexes containing lanthanide ions surrounded only by solvent are limited almost exclusively to aqueous systems. For example, $[Ln(H_2O)_x]^{3+}$ ions have been identified in systems such as $[Sm(H_2O)_9]Br_3(dioxane)_2$,[52] $[Ln(H_2O)_8]$-

Table 3. Selected Bond Distances (Å) and Angles (deg) for $\{[(N\text{-}MeIm)_4Sm(\mu\text{-}OH)]_3(\mu_3\text{-}OH)_2\}I_4$ (**6**) (for Sm(1) Only) and $[(N\text{-}MeIm)_5Sm(\mu\text{-}OH)]_2I_4$ (**7**)

6		**7**	
Sm(1)–O(1)	2.454(9)	Sm(1)–O(1)	2.309(3)
Sm(1)–O(2)	2.435(9)	Sm(1)–O(1′)	2.287(3)
Sm(1)–O(3)	2.347(10)		
Sm(1)–O(5)	2.323(11)		
Sm(1)–N(1)	2.631(12)	Sm(1)–N(1)	2.562(4)
Sm(1)–N(3)	2.554(15)	Sm(1)–N(3)	2.531(4)
Sm(1)–N(5)	2.610(14)	Sm(1)–N(5)	2.534(4)
Sm(1)–N(7)	2.583(14)	Sm(1)–N(7)	2.504(4)
		Sm(1)–N(9)	2.591(4)
O(1)–Sm(1)–O(2)	60.3(3)	O(1)–Sm(1)–O(1′)	68.4(1)
O(1)–Sm(1)–O(3)	73.3(3)	Sm(1)–O(1)–Sm(1′)	111.0(1)
O(2)–Sm(1)–O(3)	70.0(3)		
O(1)–Sm(1)–O(5)	71.4(3)		
O(2)–Sm(1)–O(5)	72.5(3)		
O(3)–Sm(1)–O(5)	137.6(3)		
O(1)–Sm(1)–N(1)	137.1(4)	O(1)–Sm(1)–N(1)	120.6(1)
O(2)–Sm(1)–N(1)	134.3(4)	O(1)–Sm(1)–N(3)	116.9(1)
O(3)–Sm(1)–N(1)	145.1(4)	O(1)–Sm(1)–N(5)	79.1(1)
O(5)–Sm(1)–N(1)	77.0(4)	O(1)–Sm(1)–N(7)	79.1(1)
O(1)–Sm(1)–N(3)	74.4(4)	O(1)–Sm(1)–N(9)	146.7(1)
O(2)–Sm(1)–N(3)	134.7(4)	N(1)–Sm(1)–O(1′)	79.1(1)
O(3)–Sm(1)–N(3)	97.9(4)	N(3)–Sm(1)–O(1′)	83.7(1)
O(5)–Sm(1)–N(3)	94.5(4)	N(5)–Sm(1)–O(1′)	127.9(1)
O(1)–Sm(1)–N(5)	130.3(4)	N(7)–Sm(1)–O(1′)	125.3(1)
O(2)–Sm(1)–N(5)	134.4(5)	N(9)–Sm(1)–O(1′)	144.7(1)
O(3)–Sm(1)–N(5)	72.8(4)		
O(5)–Sm(1)–N(5)	149.5(4)		
O(1)–Sm(1)–N(7)	135.9(4)		
O(2)–Sm(1)–N(7)	75.6(4)		
O(3)–Sm(1)–N(7)	92.2(4)		
O(5)–Sm(1)–N(7)	97.1(4)		
N(1)–Sm(1)–N(3)	80.1(4)	N(1)–Sm(1)–N(3)	106.8(1)
N(1)–Sm(1)–N(5)	73.0(4)	N(1)–Sm(1)–N(5)	152.7(1)
N(3)–Sm(1)–N(5)	75.5(5)	N(3)–Sm(1)–N(5)	75.9(1)
N(1)–Sm(1)–N(7)	75.4(4)	N(1)–Sm(1)–N(7)	81.5(1)
N(3)–Sm(1)–N(7)	149.6(4)	N(3)–Sm(1)–N(7)	151.0(1)
N(5)–Sm(1)–N(7)	80.4(4)	N(5)–Sm(1)–N(7)	84.4(1)
		N(1)–Sm(1)–N(9)	76.8(1)
		N(3)–Sm(1)–N(9)	79.1(1)
		N(5)–Sm(1)–N(9)	77.0(1)
		N(7)–Sm(1)–N(9)	75.8(1)

(51) Tan, G. O.; Hodgson, K. O.; Hedman, B.; Clark, G. R.; Garrity, M. L.; Sorrell, T. N. *Acta Crystallogr.* **1990**, *C46*, 1773–1775.

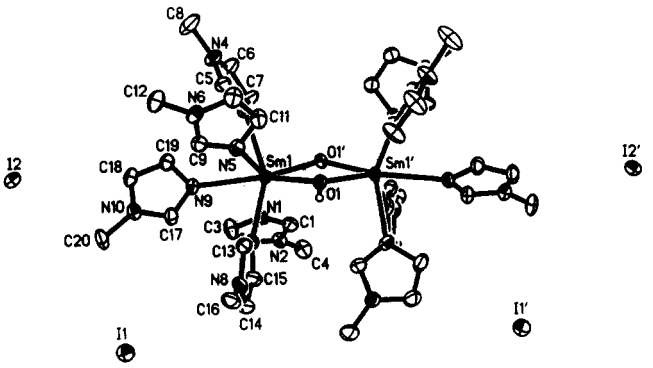

Figure 7. Thermal ellipsoid plot of $[(N\text{-MeIm})_5Sm(\mu\text{-OH})]_2I_4$ (**7**), drawn at the 50% probability level.

Cl_3(crown ether) (Ln = Nd, Gd, Dy, Y, Lu),[53] and $[Ln(H_2O)_8]Cl_3$(4,4′-bipyridine) (Ln = Gd, Y).[54] However, it is more common for lanthanide halides to crystallize as $[LnX_2(solvate)_x]^+$ species in which only one halide is a detached counterion.[55] In nonaqueous solvents such as THF, NH_3, and DME, lanthanide halides typically crystallize as seven-coordinate $LnX_3(solvent)_4$ complexes in which all three halides are bound to the metal.[56] However, displacement of one iodide ligand was observed in $[SmI_2(OPMePh_2)_4]I$.[34] The fact that *N*-MeIm readily displaces all of the ligands and provides a highly solvated complex which is stable enough to be characterized by X-ray crystallography shows that this solvent offers some special opportunities in trivalent lanthanide chemistry. For example, *N*-MeIm may be quite useful in displacing ligands other than halides from trivalent lanthanide metal centers when dissociation of the ligand is desirable.

The *N*-MeIm ligand does not appear to have as great an affinity for Sm(II) as it does for Sm(III), since upon crystallization of **1**, 1 equiv of *N*-MeIm is lost per samarium and SmI_2 crystallizes as the six-coordinate species, **2**, with only three *N*-MeIm ligands in its coordination sphere. An analogous result is observed for europium. Nevertheless, *N*-MeIm is successful in providing a crystallographically characterizable SmI_2 complex which is noteworthy since, despite the extensive use of $SmI_2(THF)_2$ in organic synthesis,[9,10] relatively few SmI_2 complexes have been fully characterized by X-ray studies.[30,33] Moreover, *N*-MeIm does appear to solvate Sm(II) better than *tert*-butyl cyanide since "SmI_2/*N*-MeIm" crystallizes as the trisolvated dimer **2** rather than as the disolvated polymer $[Sm(\mu\text{-}I)_2(NCCMe_3)_2]_n$ (**8**).

The isolation of $\{[(N\text{-MeIm})_4Sm(\mu\text{-OH})]_3(\mu_3\text{-OH})_2\}I_4$ (**6**) and $[(N\text{-MeIm})_5Sm(\mu\text{-OH})]_2I_4$ (**7**) shows other ways in which *N*-MeIm can be used productively with the lanthanides. These structures show that the *N*-MeIm ligand has the capacity to stabilize samarium complexes of the small hydroxide ligand. Hydroxide complexes comprise only a small percentage of fully characterized compounds in lanthanide chemistry,[13-22] although hydrolytic decomposition, which is likely to have hydroxide intermediates, is a common process with these metals. Hydroxide complexes may be more readily available using *N*-MeIm. More generally, *N*-MeIm may be a good solvent with which to stabilize complexes of other ligands which are difficult to isolate on lanthanide metal centers. Complexes **6** and **7** suggest that an accessible hydroxide-based polymetallic chemistry may now be available to the lanthanides whereas, in the past, polymetallic lanthanide chemistry involved primarily alkoxide ligands.

It is interesting to note that the hydroxide complexes **6** and **7** constitute a pair of compounds analogous to the $(Cp_2LnZ)_2$[57,58] and $\{[(Cp_2LnZ)_3]H\}^-$[48,58,59] cyclopentadienyl series (Z = H, OMe). In this sense, the set of four *N*-MeIm ligands in **6** and the set of five *N*-MeIm ligands in **7** are taking the place of the bis(cyclopentadienyl) ligand set so common with the lanthanide metals.[57] Such bimetallic–trimetallic pairs are not as common for lanthanide alkoxide complexes since a given ligand size usually generates either a trimetallic structure (for example with *tert*-butoxide ligands[12,44-47]) or mono- and bimetallic complexes (e.g. with $OCH(CMe_3)_2$[60] and 2,6-dialkylphenols[61]).[62] It may be that the *N*-MeIm ligand is better able to stabilize a variety of nuclearities than the coordinating solvents previously used for these metals. The fact that four *N*-MeIm ligands are used for this purpose in **6** and five in **7** and the variable ability of *N*-MeIm to fill the coordination spheres in **2** and **5** (Figure 4) suggest that a set of *N*-MeIm ligands can be used to satisfy the steric needs of the rest of the complex more precisely than two cyclopentadienyl ligands.

Conclusion

As in other areas of metal-based chemistry, the *N*-methylimidazole ligand appears to offer special opportunities for the lanthanide metals. The strong donor capacity of this monodentate ligand provides new opportunities to develop the coordination environments of the lanthanides. Further investigation of *N*-MeIm in lanthanide chemistry is clearly warranted.

Acknowledgment. We thank the National Science Foundation for support of this research and the Stiftung Stipendien-Fonds des Verbandes der Chemischen Industrie, Germany, for the award of a Liebig fellowship (to G.W.R.).

Supplementary Material Available: Textural details of the collection of X-ray diffraction data and solution and refinement of the structures and tables of crystal data, positional parameters, bond distances and angles, and thermal parameters (65 pages). Ordering information is given on any current masthead page.

(52) Barnes, J. C.; Nicoll, G. Y. R. *Inorg. Chim. Acta* **1985**, *110*, 47–50.
(53) (a) Rogers, R. D.; Kurihara, L. K. *Inorg. Chim. Acta* **1986**, *116*, 171–177. (b) Rogers, R. D.; Kurihara, L. K. *Inorg. Chim. Acta* **1987**, *129*, 277–282. (c) Rogers, R. D.; Kurihara, L. K. *Inorg. Chim. Acta* **1987**, *130*, 131–137. (d) Rogers, R. D. *Inorg. Chim. Acta* **1987**, *133*, 347–352. (e) Rogers, R. D. *Inorg. Chim. Acta* **1988**, *149*, 307–314. (f) Rogers, R. D. *J. Coord. Chem.* **1988**, *16*, 415–424.
(54) (a) Bukowska-Strzyzewska, M.; Tosik, A. *Acta Crystallogr.* **1982**, *B38*, 265–267. (b) Bukowska-Strzyzewska, M.; Tosik, A. *Acta Crystallogr.* **1982**, *B38*, 950–951.
(55) (a) Rogers, R. D. *Inorg. Chim. Acta* **1988**, *149*, 307–314. (b) Urland, W.; Schwanitz-Schuller, U. *Angew. Chem., Int. Ed. Engl.* **1983**, *22*, 1009–1010.
(56) Radonovich, L. J.; Glick, M. D. *J. Inorg. Nucl. Chem.* **1973**, *35*, 2645–2752. Castellani, C. B.; Tazzoli, V. *Acta Crystallogr.* **1984**, *C40*, 1832–1834. Castellani, C. B.; Coda, A. *Acta Crystallogr.* **1985**, *C41*, 186–189. Ning-Hai, H.; Yong-Hua, L.; Qi, S.; Yan, X.; En-Dong, S. *Acta Chim. Sinica (Engl. Ed.)* **1986**, *44*, 388. Wenqi, C.; Zhongsheng, X. Y.; Yuguo, F.; Guangdi, Y. *Inorg. Chim. Acta* **1987**, *130*, 125–129. Rogers, R. D.; Voss, E. J.; Etzenhouser, R. D. *Inorg. Chem.* **1988**, *27*, 533–542. Zhongsheng, J.; Guojin, N.; Ninghai, H.; Wenqi, C. *Yingyo Huaxue (Chin. J. Appl. Chem.)* **1989**, *6*, 68. Lin, S.-H.; Dong, Z.-C.; Huang, J.-S.; Zhang, Q.-E.; Lu, X.-L. *Acta Crystallogr.* **1991**, *C47*, 426–427.
(57) Evans, W. J. *Polyhedron* **1987**, *6*, 803–835. Marks, T. J.; Ernst, R. D. In *Comprehensive Organometallic Chemistry*; Wilkinson, G., Stone, F. G. A., Abel, E. W., Eds.; Pergamon Press: London, 1982; Chapter 21. Schumann, H.; Genthe, W. In *Handbook on the Physics and Chemistry of Rare Earths*; Gschneidner, K. A., Jr., Eyring, L., Eds.; Elsevier: Amsterdam, 1985; Vol. 7, Chapter 53 and references therein.
(58) Evans, W. J.; Sollberger, M. S.; Shreeve, J. L.; Olofson, J. M.; Hain, J. H., Jr.; Ziller, J. W. *Inorg. Chem.* **1992**, *31*, 2492–2501.
(59) Evans, W. J.; Meadows, J. H.; Wayda, A. L.; Hunter, W. E.; Atwood, J. L. *J. Am. Chem. Soc.* **1982**, *104*, 2015–2017. Evans, W. J.; Meadows, J. H.; Hanusa, T. P. *J. Am. Chem. Soc.* **1984**, *106*, 4454–4460. Evans, W. J.; Drummond, D. K.; Hanusa, T. P.; Doedens, R. J. *Organometallics* **1987**, *6*, 2279–2285.
(60) Stecher, H. A.; Sen, A.; Rheingold, A. *Inorg. Chem.* **1989**, *28*, 3280–3282.
(61) Evans, W. J.; Olofson, J. M.; Ziller, J. W. *Inorg. Chem.* **1989**, *28*, 4308–4309. Hitchcock, P. B.; Lappert, M. F.; Smith, R. G. *Inorg. Chim. Acta* **1987**, *139*, 183–184. Deacon, G. B.; Hitchcock, P. B.; Holmes, S. A.; Lappert, M. F.; MacKinnon, P.; Newnham, R. H. *J. Chem. Soc., Chem. Commun.* **1989**, 935–937. Stecher, H. A.; Sen, A.; Rheingold, A. L. *Inorg. Chem.* **1988**, *27*, 1130–1132. Deacon, G. B.; Feng, T.; MacKinnon, P.; Newnham, R. H.; Nickel, S.; Skelton, B. W.; White A. H. *Aust. J. Chem.* **1993**, *46*, 387–399.
(62) The cationic *tert*-butoxide complexes $[Y_3(OR)_7Cl(THF)_3]^+$ and $[Y_2(OR)_4Cl(THF)_4]^+$ are rare examples in which both bimetallic and trimetallic complexes were crystallographically characterized.[46]